

1
2 **Orographic effect on extreme precipitation statistics peaks at hourly time scales**
3

4 **Francesco Marra^{1,2}, Moshe Armon², Marco Borga³, Efrat Morin²**

5 ¹Institute of Atmospheric Sciences and Climate, National Research Council of Italy, Bologna,
6 Italy.

7 ²The Fredy & Nadine Herrmann Institute of Earth Sciences, the Hebrew University of Jerusalem,
8 Israel.

9 ³Department of Land Agriculture Environment and Forestry, University of Padua, Italy.

10
11 Corresponding author: Francesco Marra (f.marra@isac.cnr.it, marra.francesco@mail.huji.ac.il)
12

13 **Key Points:**

- 14 • Orography negligibly affects tail heaviness of 10-minute intensity and decreases it for
15 longer durations with a minimum around 1 hour
- 16 • The “reverse orographic effect” previously observed for hourly extremes is found to be
17 more marked at sub-hourly durations
- 18 • Breaking of scale-invariance at sub-hourly durations in mountainous areas bares
19 important implications for risk management
20

Abstract

Orographic impact on extreme sub-daily precipitation is critical for risk management but remains insufficiently understood due to complicated atmosphere-orography interactions and large uncertainties. We investigate the problem adopting a framework able to reduce uncertainties and isolate the systematic interaction of Mediterranean cyclones with a regular orographic barrier. The average decrease with elevation reported for hourly extremes is found enhanced at sub-hourly durations. Tail heaviness of 10-minute intensities is negligibly affected by orography, suggesting self-similarity of the distributions at the convective scale. Orography decreases the tail heaviness at longer durations, with a maximum impact around hourly scales. These observations are explained by an orographically-induced redistribution of precipitation towards stratiform-like processes, and by the succession of convective cores in multi-hour extremes. Our results imply a breaking of scale-invariance at sub-hourly durations, with important implications for natural hazards management in mountainous areas.

34

Plain Language Summary

Preparedness to natural hazards in mountainous areas strongly relies on the knowledge of extreme rainfall probability. The presence of mountains influences the motion of air masses, thereby modifying the storms characteristics. Here, we use a novel approach to quantify the impact of mountains on the probability of occurrence of extreme rainfall of short duration. We find that mountains tend to decrease the mean annual maximum intensities at sub-hourly scales and tend to decrease the extremely high intensities, such as the events occurring on average once in 100 years. The second effect is however non-monotonic, in that it grows between 10 minute and 1 hour and diminishes between 1 and 6 hours. This means that sub-hourly extremes could be higher than what we can estimate from hourly data, and implies that statistical methods typically adopted for risk assessment may systematically underestimate the risk of short-duration extremes.

47 **1 Introduction**

48 In mountainous regions, preparedness to precipitation driven natural hazards such as flash
49 floods and debris flows, strongly relies on the quantitative knowledge of extreme precipitation of
50 short duration (Borga et al., 2014). In particular, rare yearly exceedance probabilities are crucial
51 for risk assessment and management (Chow et al., 1988). This information is traditionally
52 derived from observations using statistical methods based on the sampled extremes and are thus
53 subject to large stochastic and sampling uncertainties that reduce our ability to understand the
54 underlying processes and predict the local responses to climate change (Fatichi et al., 2016). The
55 methods typically adopted to decrease these uncertainties entail the pooling of information from
56 multiple sources; either spatially, from homogeneous regions, and/or temporally, by assuming
57 scale-invariance of extreme precipitation across durations (Buishand, 1991; Burlando and Rosso,
58 1996). Drawback of these methods is the need for assumptions that may mask inter-station and
59 inter-duration effects (Furcolo et al., 2016).

60 Orography physically bounds the atmospheric air motion inducing ascent of air parcels,
61 generating atmospheric waves and, therefore, affecting the precipitation processes (Bonacina,
62 1945; Roe, 2005). The impact of orography on long-duration precipitation (i.e., daily or multi-
63 day) is quite well understood, with an increase of the yield along the windward slope due to the
64 lifting of air masses, and a decrease in the lee side slopes because of air descent and drying;
65 overall, a typically positive net impact is reported, the so-called “orographic enhancement”.
66 Conversely, the picture for sub-daily extremes is less clear (Haiden et al., 1992; Nykaken and
67 Harris, 2003; Rossi et al., 2020). Among the research efforts on the orographic effect on extreme
68 short-duration precipitation, only few studies focused on the right-tail statistics and yearly
69 exceedance probabilities. Investigations based on hourly rain gauges reported that short-duration
70 annual maxima at higher elevations were characterized by lighter-tails, and highlighted the
71 presence of a “reverse orographic effect”, that is the mean annual maxima for hourly durations
72 was found to decrease with elevation, opposing the orographic enhancement of longer duration
73 amounts (Allamano et al., 2009; Avanzi et al., 2015). However, possible varying effects on the
74 right-tail characteristics across durations could not be thoroughly examined due to the scale-
75 invariance assumptions adopted, and no information could be derived for sub-hourly durations
76 due to the lack of sufficiently long data records. Further, the presence of multiple types of

77 precipitating systems, which may interact differently with orography, and of multiple directions
 78 of advection, complicates these analyses (Picard and Mass, 2017; Marra et al., 2019).

79 The objective of this study is to improve our understanding of the orographic impact on
 80 the statistics of short duration extreme precipitation. Specifically, we quantify the impact of
 81 orography on the right-tail statistics of sub-daily and sub-hourly precipitation, and investigate the
 82 underlying statistical mechanisms. To do so, we adopt an analytical framework in which effects
 83 related to the contribution of multiple precipitating systems and advection directions are removed
 84 by isolating unique atmosphere-orography interaction conditions, and stochastic uncertainties
 85 inherent in the observation of extremes are reduced without requiring scaling/homogeneity
 86 assumptions. In this manner we are able to perform right-tail statistical analyses directly on sub-
 87 hourly records using relatively few years of data.

88 **2 Methodology**

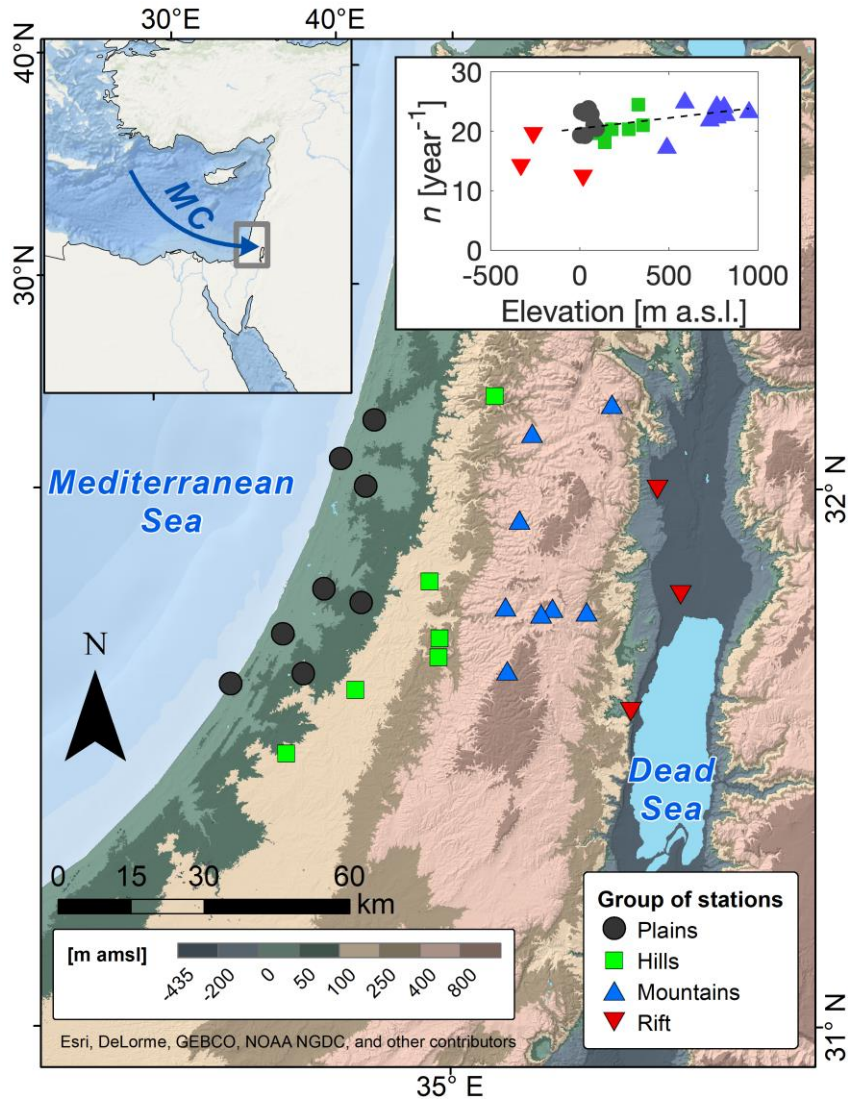
89 Novel approaches permit to quantify the yearly probability of exceedance of extremes by
 90 explicitly considering that they are finite independent samples of a stochastic process of interest,
 91 the so-called ordinary events (Marani and Ignaccolo, 2015). Under the assumption that the
 92 cumulative distribution function of the ordinary events $F(\cdot)$ is known, it is possible to quantify
 93 yearly non-exceedance probabilities ζ of extreme intensities x as: $\zeta(x) \simeq F(x)^n$, where n is the
 94 average yearly number of ordinary events (Marra et al., 2019). This approach allows considering
 95 multiple types of ordinary events contributing to the generation of extremes, such as events
 96 associated to different atmospheric circulations or precipitation processes. In this case, the yearly
 97 non-exceedance probabilities can be written as: $\zeta(x) \simeq \prod_{i=1}^S [F_i(x)]^{n_i}$, where $F_i(\cdot)$ is the
 98 cumulative distribution function of the i -th of S types of ordinary events, and n_i is the
 99 corresponding average yearly number (Marra et al., 2019; Miniussi et al., 2020).

100 While daily precipitation ordinary events are well described by Weibull distributions
 101 (Marani and Ignaccolo, 2015; Zorretto et al., 2016), sub-daily intensities follow more general
 102 distributions that are, however, Weibull right-tail equivalent (Papalexiou, 2018; Papalexiou et al.,
 103 2018; Marra et al., 2020). It is thus possible to describe a portion of their distribution which
 104 includes extremes using a two-parameter distribution in the form $F(x; \lambda, \kappa) = 1 - e^{-\left(\frac{x}{\lambda}\right)^\kappa}$, where
 105 x is the precipitation intensity of interest, and λ and κ are the scale and shape parameters,
 106 respectively. The shape parameter, in particular, determines the tail heaviness, with heavier tails

107 for smaller shapes and vice versa. The tail of the extreme value distribution $\zeta(x)$ is then
108 modulated by number of yearly events, with decreasing heaviness at increasing number of yearly
109 events, and vice versa. When defined consistently across durations, the ordinary events share
110 some of the statistical properties of annual maxima (Marra et al., 2020) but, since much larger in
111 number, the stochastic uncertainty in the analysis of their tails is reduced. In this way, reliable
112 estimates of intensities characterized extremely low yearly exceedance probability can be
113 obtained from short records (Zorzetto et al., 2016; Marra et al., 2018).

114 Here, we focus on the right-tail statistics of ordinary events which interact with
115 orography in a prescribed, systematic way. We examine a region of the southeastern
116 Mediterranean, characterized by Mediterranean climate (cold wet winter, warm dry summer), in
117 which a regular physiographic structure parallels the shoreline (Fig. 1): coastal plains, lowland
118 hills raising to a moderate mountain range (<1000 m a.s.l.), and a deep rift valley including the
119 lowest point on Earth (currently ~430 m below the sea level), the Dead Sea. East of the
120 mountains, the steep orography towards the rift causes a rain shadow desert with a sharp gradient
121 to semi-arid and arid climate (Kushnir et al., 2017). Mediterranean cyclones account for 75-90%
122 of the precipitation amount in the area and move inland along westerly tracks roughly
123 perpendicular to the orographic barrier (Alpert et al., 1990; Armon et al., 2019). The rest of
124 precipitation is associated to systems typically extending from the south and interacting with
125 orography in an irregular way (de Vries et al., 2013; Armon et al., 2018). Almost all the
126 precipitation caused by Mediterranean cyclones is associated to low-level clouds; low-level
127 flows pass the warm waters of the Mediterranean, lowering the static stability of air parcels,
128 triggering convection, and causing precipitation to reach the ground in liquid phase with only
129 sporadic snowfall. Previous studies tested the use of ordinary events for precipitation frequency
130 analyses in this region, demonstrating the robustness of the assumptions and the ability of the
131 framework to reproduce extremes from relatively short records (Marra et al., 2019; Marra et al.,
132 2020).

133



134
 135 **Figure 1.** Map of the study region detailing orography, typical direction of advection of Mediterranean
 136 cyclones (MC) in the area, and location of the rain gauges used in the study. The inset shows the average
 137 yearly number of ordinary events as a function of elevation; the slope derived from the uphill stations (rift
 138 stations are excluded) is superimposed and statistically significant (p-value 0.04).

139

140 Precipitation data are collected for 25 quality-controlled automatic tipping bucket rain
 141 gauges in a latitudinal strip across the region ($\sim 31.5\text{--}32.2^\circ\text{N}$). The instruments have a resolution
 142 of 0.1 mm per tip and automatically record data every 10 minutes. Data are organized by
 143 hydrologic years (September 1 to August 31) and years with more than 10% missing data are
 144 discarded. The records span 9-26 years (17.0 ± 4.7 yr). To aid the analyses, the stations are
 145 organized into four groups according to the local physiography (Fig. 1): plains (west of the

146 mountains, elevation $z < 100$ m a.s.l.), hills ($100 < z \leq 400$ m a.s.l.), mountains ($z > 400$ m
147 a.s.l.), rift (east of the mountains, $z < 50$ m a.s.l.).

148 Following previous studies in similar climates (Restrepo-Posada and Eagleson, 1982;
149 Marra et al., 2020), independent storms are defined as consecutive wet (≥ 0.1 mm/10 min) time
150 intervals separated by 6-hour dry hiatuses; short (< 30 min) storms are removed to avoid noise
151 due to individual tips of the rain gauge. Storms associated to Mediterranean cyclones are isolated
152 according to a semi-objective synoptic classification (Alpert et al., 2004), as detailed in Table
153 S1; as the classification is daily, the time in which each storm ends is used. Ordinary events are
154 computed as the maximum intensities observed within each storm using moving windows of
155 durations between 10 minutes and 6 hours (10, 20, 30 min, 1, 2, 3, 6 hours) (Marra et al., 2020).
156 The ordinary events' right-tail is defined as the Weibull-identically-distributed portion of the
157 events; in our region this was identified as the largest 25% of the ordinary events (Marra et al.,
158 2019; Marra et al, 2020). The scale and shape parameters of the Weibull distributions describing
159 the ordinary events are computed left-censoring the remaining portion of the data, that is without
160 considering the intensities but retaining the weight in probability, and using a least squares
161 regression in Weibull-transformed coordinates (Marani & Ignaccolo, 2015). The number of
162 events per year is computed as the arithmetic mean of the yearly number of ordinary events.
163 Despite the relatively short records, given the number of yearly ordinary events (Fig. 1), the two
164 parameters describing their right tails are estimated using between ~ 40 and over 150 data points,
165 with clear advantages in estimation accuracy over traditional extreme value methods in which
166 one/few events per year are used and three parameters are sought.

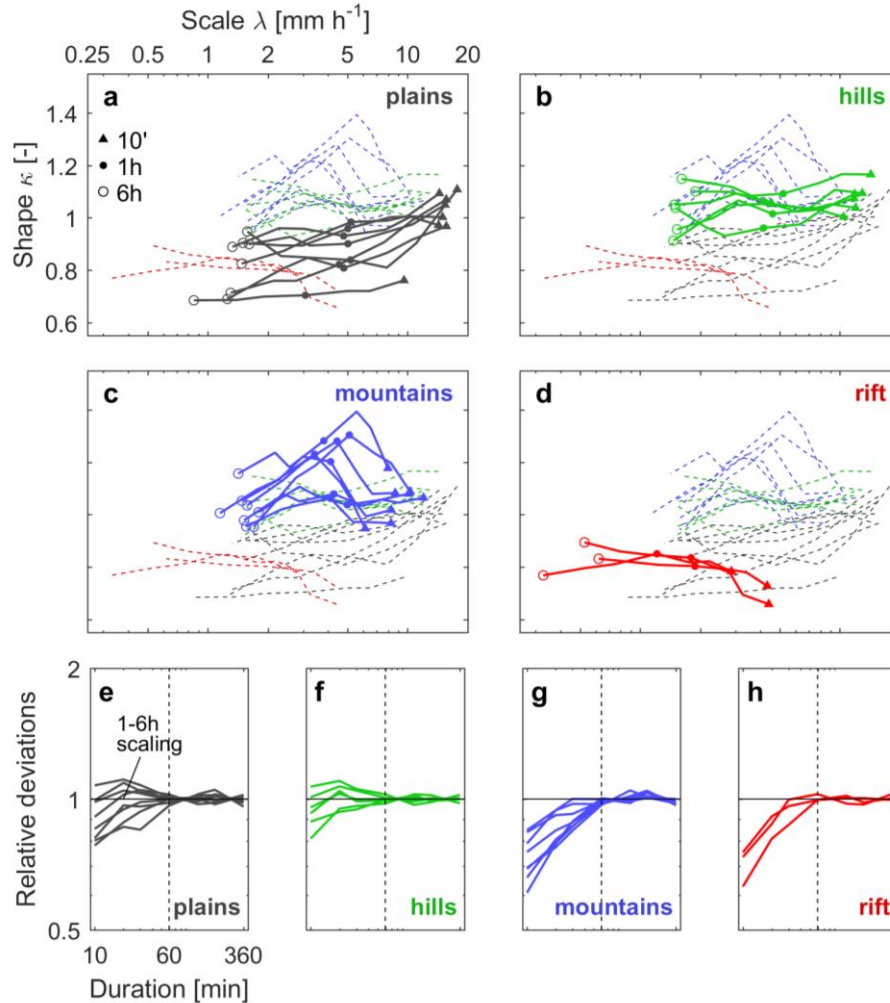
167 The impact of terrain elevation on the parameters and number of yearly events is
168 examined using the non-parametric Sen's slope estimator and the slope significance (0.05
169 significance level) is tested using the Mann-Kendall test (Haan, 2002). No serial correlation in
170 the data is expected. The stations downwind of orography are affected by a different orographic
171 effect, and are too few and sparse to represent the steep gradient on lee side of the mountain
172 range. Rift stations are thus shown in the figures for a qualitative description of the downwind
173 effect, but are not used for these statistical analyses.

174 **3 Results and Discussion**

175 The events occurrence frequency is weakly ($3.6 \text{ events km}^{-1}$) but significantly (p-value
176 0.04) affected by orography (Fig. 1), with some of the variance possibly explained by latitude
177 (Armon et al., 2019). On the lee side of the mountain range, the descent of dry air induced by
178 orography drastically decreases the yearly numbers. The shape parameter of the ordinary events
179 right-tail distribution (Fig. 2 a-d) decreases with duration in the plains and, less markedly, in the
180 hills, indicating heavier-tailed distributions at longer durations. This confirms what found in
181 Marra et al. (2020) in a coastal region at slightly higher latitude. Conversely, a non-monotonic
182 behavior of the shape is observed in the mountains, with increasing shape parameter, hence
183 lighter tails, at longer durations, and a maximum around durations of 1 hour. In the downwind
184 rift the shape smoothly increases with duration, indicating heavier-tails at shorter durations.
185 Estimating annual maxima from 10-minute data in the region yields 11% and 6%
186 underestimation for 10- and 20-minute durations, respectively (Marra and Morin, 2015). This
187 underestimation does not depend on the intensity, and is thus expected to affect the scale
188 parameter only, with no systematic impact on the shape parameter. Additionally, as based on
189 ordinary events our results for short durations are expected to be less affected by saturation of the
190 tipping bucket devices at high intensities with respect to results based on traditional analyses of
191 extremes.

192 The non-monotonic dependence of the tail with duration observed in the mountains and,
193 to some extent, in the rift implies a violation of the scale-invariance, assumption often adopted in
194 the analysis of extremes, at sub-hourly durations. This is highlighted in Fig. 2 e-h, where the
195 relative deviations of the scale parameter from the power-law relations computed for durations
196 exceeding 1 hour, are shown (see also Fig. S2); this is the time interval in which the power-law
197 behavior generally holds more robustly (Burlando and Rosso, 1996; Ceresetti et al., 2010), and in
198 which the systematic underestimations due to the use of 10-minute blocks are negligible.
199 Interestingly, these deviations concern all sub-hourly durations and pertain regions in which, on
200 average, the 10-minute peak intensities are lower, so that they cannot be explained by
201 measurement effects related to the saturation of the tipping bucket rain gauge at high intensities.

202



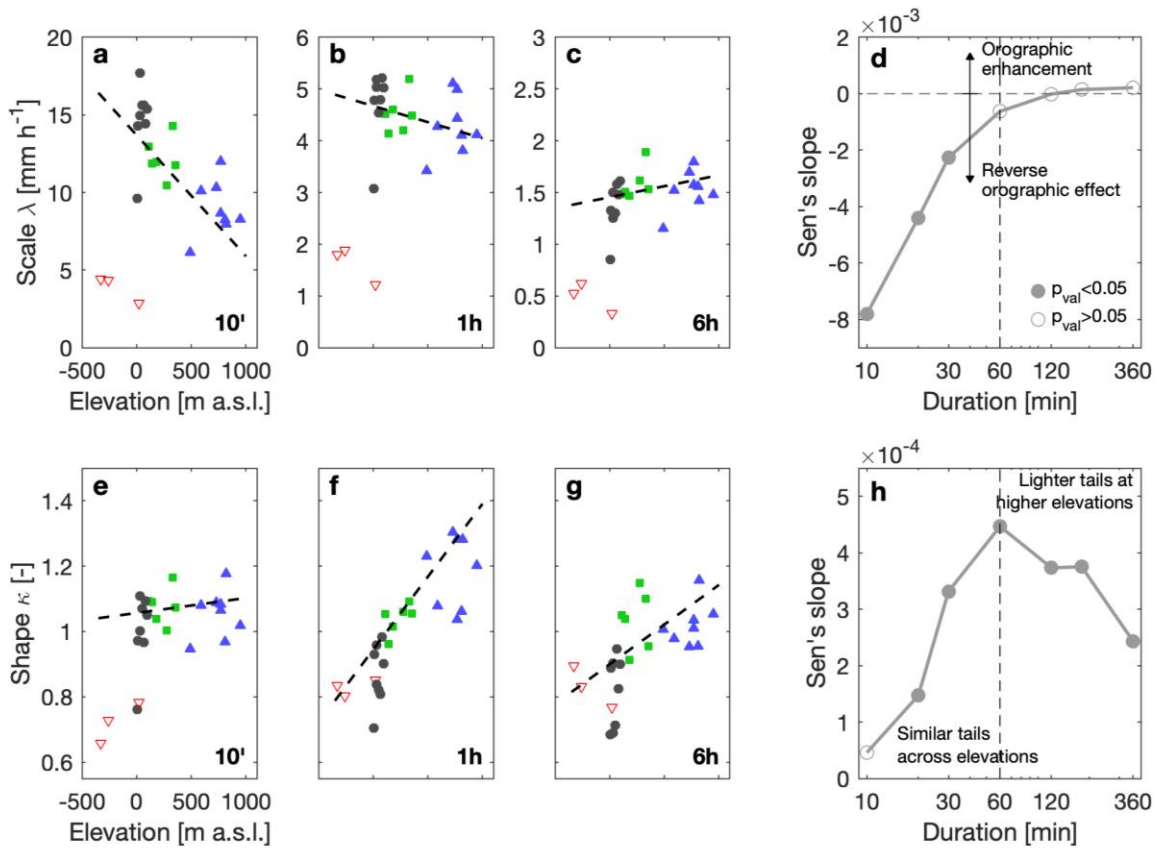
203

204 **Figure 2.** (a-d) Parameters of the distributions describing the right tail of the ordinary events over the four
 205 regions for durations of 10, 20, 30 minutes, 1, 2, 3, 6 hours; durations of 10 minutes, 1 hour and 6 hours
 206 are marked with triangles, dots and circles, respectively. Parameters of the other regions are dashed in the
 207 background to aid visual comparison. (e-h) Relative deviations of the scale parameters from the scale-
 208 duration power-law relations computed for 1-6 hours time interval.

209

210 The case of non-systematic atmosphere-orography interaction (that is, all the non-Mediterranean-
 211 cyclone events) is shown as a control case in the supplementary Figure S1; here, plains, hills and
 212 mountains all share similar parameters and behaviors, with lighter-tailed distributions at shorter
 213 durations. This shows that isolating systematic interactions is crucial to understand the
 214 mechanisms behind the orographic impact on precipitation right-tail characteristics, and confirms
 215 that what shown in Fig. 2 is an effect related to the interaction of westerlies induced by
 216 Mediterranean cyclones with the local terrain.

217



218

219 **Figure 3.** (a-c) Scale parameters of the Weibull distributions describing the ordinary events right-tail for
 220 durations of 10 minutes, 1 hour and 6 hours as a function of elevation; approximations of the relations
 221 between scale parameter and elevation for the uphill stations (rift stations are excluded) are shown as
 222 dashed lines. (d) Sen's slope of the scale-elevation relations as a function of duration; statistically
 223 significant slopes are shown as full dots. (e-g) Shape parameters of the Weibull distributions describing
 224 the ordinary events right-tail for durations of 10 minutes, 1 hour and 6 hours as a function of elevation;
 225 approximations of the relations between shape parameter and elevation for the uphill stations (rift stations
 226 are excluded) are shown as dashed lines. (h) Sen's slope of the shape-elevation relations as a function of
 227 duration; statistically significant slopes are shown as full dots.

228

229 The relation between terrain elevation and scale and shape parameters describing the
 230 right-tail of ordinary events is shown in Fig. 3, for durations of 10 minutes, 1 hour and 6 hours.
 231 The slope of the relations between scale parameter and elevation for the uphill stations changes
 232 sign between durations of 1 and 2 hours, with statistically significant negative slopes for sub-
 233 hourly durations. Non-statistically-significant slopes are reported for hourly (negative slope) and

234 multi-hour (positive slope) intensities. This indicates that sub-hourly ordinary events are
235 typically larger at lower elevations, and become weaker with increasing elevation: it is the
236 “reverse orographic effect” reported by Allamano et al. (2009) and Avanzi et al. (2015) for
237 hourly durations. Our results prove this is not an artifact introduced by the use of hourly data to
238 estimate hourly extremes, and suggest that the effect is enhanced and more significant at shorter
239 durations.

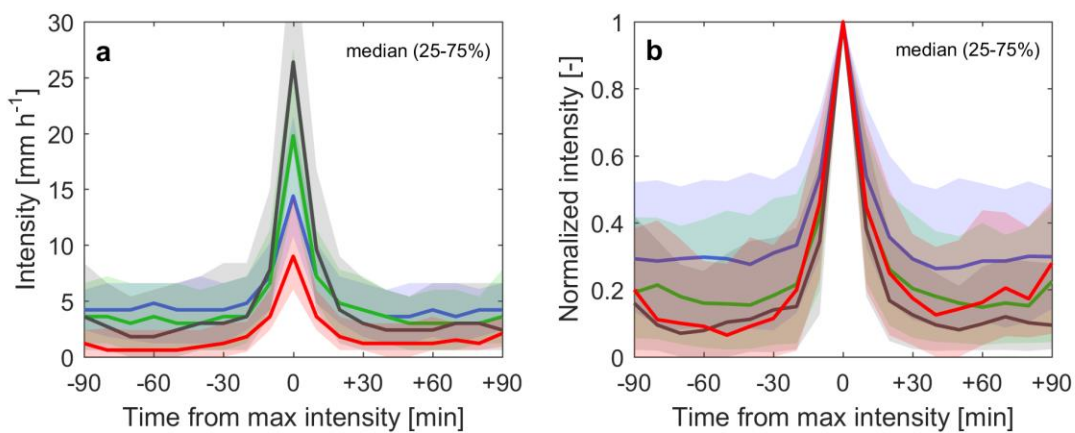
240 Notwithstanding, the shape parameter shows a peculiar behavior with elevation, with
241 opposing trends for sub-hourly and multi-hour durations. No significant dependence on elevation
242 can be identified at 10-minute duration, while longer durations present statistically significant
243 positive slopes, implying lighter tails at higher elevation. More specifically, the slopes increase
244 between 10 minutes and 1 hour and decreases for durations between 1 and 6 hours. This means
245 that for increasing durations up to 1 hour, higher elevations are characterized by increasingly
246 lighter-tailed distributions. For multi-hour durations the effect diminishes and the dependence on
247 elevation becomes less marked, even if still significant.

248 These observations imply that the tail heaviness of very-short-duration (10 minutes)
249 processes is not strongly impacted by orography, suggesting a degree of self-similarity in the
250 distributions of convective-scale processes. Conversely, orography plays a prominent role in the
251 way the instantaneous intensities aggregate in time, which impacts the tail heaviness in a non-
252 monotonic way. The effect is related to the way orography affects the temporal organization of
253 extremes. Extreme short-duration intensities are decreased by elevation and the temporal
254 structure of the precipitation time series is smoothed (Fig. 4). This confirms previous
255 observations on the characteristics of convective precipitation in the area (Peleg and Morin,
256 2012), and is likely related to a redistribution of precipitation towards stratiform-like processes
257 surrounding the convective cores induced by the orographic lifting of air masses (Houze et al.,
258 2001; Bongioannini Cerlini et al., 2005). The temporal autocorrelation structure and the fraction
259 of wet time intervals observed around the intensity peaks support this observation (Fig. S3). At
260 very short time scales, extremes essentially consist in convective cores. As duration increases,
261 the surrounding stratiform-like processes start contributing, and then, further increasing duration,
262 possible sequences of convective cores (e.g., Roe, 2005). For multi-hour durations, this causes
263 the well-known “orographic enhancement” while hourly time scales are probably long enough to

264 include the stratiform-like processes but not enough to include the sequences convective cores
 265 (Peleg and Morin, 2012).

266 Orography is expected to affect various aspects of extreme precipitation differently,
 267 depending on height, slope and lateral extent of the topographic barrier, wind speed, atmospheric
 268 stability, relative humidity, and moisture fluxes, etc. (Roe, 2005). Our results are based on the
 269 unique circumstances we isolated, and the characteristic hourly time scale we report is likely
 270 related to the typical convective processes originated by Mediterranean cyclones in the region.
 271 However, these systems consist in westerly winds blowing almost perpendicularly to the
 272 mountain range (Fig. 1), low-level clouds fed by abundant moisture flux, and low-level
 273 advection from the sea. The breadth of this study is thus expected to be wider, as it represents
 274 more general cases in which low-level moisture and clouds are forced upwards by mountain
 275 barriers generating heavy rainfall along their track. For instance, similar conditions are present
 276 during atmospheric rivers at the eastern boundaries of oceanic basins (e.g., Dacre et al., 2015),
 277 extra-tropical cyclones at the eastern Atlantic Ocean or the Mediterranean (Toreti et al., 2016)
 278 and other regions of the world. Our findings suggest that, in these conditions, sub-hourly
 279 precipitation intensities in mountainous regions may be characterized by heavier tails than hourly
 280 intensities, and that the heaviness of such tails cannot be adequately quantified using scale-
 281 invariant methods. This bares important implications for risk management in mountainous areas
 282 and for the design of protection infrastructures against natural hazards related to short-duration
 283 extremes, such as debris flows and flash floods.

284



285

286 **Figure 4.** Temporal structure of extreme events. (a) Time series (median and 50% interval) of the
 287 ordinary events centered around the moment in which the maximum 10-min intensity is recorded; colors

288 refer to the physiographic region as in Fig. 1. (b) Same as in panel a, but with intensities normalized over
289 the event maximum value.

290 **4 Conclusions**

291 We quantified the impact of orography on the right-tail statistics of sub-daily and sub-
292 hourly precipitation exploiting a novel framework for the analysis of extremes based on multiple
293 types of ordinary events. In this way, we could reduce the stochastic uncertainties without
294 requiring scaling/homogeneity assumptions, and remove possible effects related to the
295 contribution of different precipitating system and advection directions. We focused on the case
296 of Mediterranean cyclones in the southeastern Mediterranean, where unique atmosphere-
297 orography interaction conditions are observed.

298 Our findings confirm the presence of a “reverse orographic effect”, previously observed
299 for hourly intensities, and suggest it could be further enhanced at shorter durations. The tail
300 heaviness at very short durations (10 minutes) seems unaffected by orography, suggesting a
301 degree of self-similarity in the distributions of convective-scale processes. Conversely,
302 orography tends to decrease the tail heaviness at longer durations, with a maximum around
303 hourly scales; in mountainous regions a non-monotonic response is observed, with decreasing
304 tail heaviness between 10 minute and 1 hour and increasing between 1 and 6 hours. This is likely
305 related to a smoothing of the events structure, possibly caused by the redistribution of
306 precipitation towards stratiform-like processes: while hourly time intervals likely include
307 individual convective cores and the related stratiform-like portion, multi-hour intervals may
308 include sequences of convective and stratiform-like elements, which aggregate and cause the
309 well-known orographic enhancement.

310 Our findings place previous observations limited to hourly durations into a wider context,
311 and add crucial knowledge for risk management in mountainous regions. In fact, the breaking of
312 scale-invariance observed around hourly durations implies a systematic underestimation of the
313 tail heaviness for sub-hourly intensities by the often-adopted scale-invariant methods. This has
314 important implications for the management of natural hazards typical of mountainous regions,
315 such as flash floods and debris flows. As based on the analysis of Mediterranean cyclones with
316 typical advection directions roughly perpendicular to the mountain range, our results are
317 quantitatively relevant for this specific study case, but are expected to represent more general
318 cases in which low-level moisture is forced by mountain barriers along the storm track, such as

319 extra-tropical cyclones and atmospheric rivers at the eastern boundaries of their oceanic basins.
320 Analysis of different regions and types of precipitating systems, and investigations based on
321 convection-permitting numerical models could improve the understanding of the physical
322 mechanisms behind the observations, and could provide improved information on short-duration
323 extremes related to multiple underlying processes. The used approach can be extended to other
324 study cases and can be used to investigate non-stationary conditions and climate change impacts
325 on extreme precipitation under orographic forcing.

326 **Acknowledgments**

327 The authors declare no conflict of interest. Precipitation data provided by the Israel
328 Meteorological Service can be retrieved from www.ims.gov.il. Codes and data produced in the
329 study are available at doi:10.5281/zenodo.4134901 and doi:10.5281/zenodo.3971558. The study
330 was funded by the Israel Science Foundation [grant no. 1069/18], the Israel Ministry of Science
331 and Technology [grant no. 61792], by JNF [grant no. 30-7-010-11], and the National Research
332 Council of Italy. This is a contribution to the HyMeX program. Authors contribution:
333 Conceptualization, paper review and editing: all authors; Funding acquisition: EM, FM; Formal
334 analyses, Data curation, Paper writing: FM.

335 **References**

- 336 Allamano, P., Claps, P., Laio, F., & Thea, C. (2009), A data-based assessment of the dependence
337 of short-duration precipitation on elevation. *Phys. Chem. Earth*, *34*, 635–641,
338 doi:10.1016/j.pce.2009.01.001
- 339 Alpert, P., Neeman, B. U., & Shay-EL, Y. (1990), Climatological analysis of Mediterranean
340 cyclones using ECMWF data. *Tellus A*, *42(A)*, 65–77, doi:10.3402/tellusa.v42i1.11860
- 341 Alpert, P., Osetinsky, I., Ziv, B., & Shafir, H. (2004), Semi-Objective Classification for Daily
342 Synoptic Systems: Application to the Eastern Mediterranean Climate Change. *Int. J.*
343 *Climatol.* *24(8)*, 1001–11, doi:10.1002/joc.1036
- 344 Armon, M., Dente, E., Smith, J. A., Enzel, Y., & Morin, E. (2018), Synoptic-scale control over
345 modern rainfall and flood patterns in the levant drylands with implications for past climates.
346 *J. Hydrometeorol.* *19*, 1077–1096
- 347 Armon, M., Morin, E., & Enzel, Y. (2019), Overview of modern atmospheric patterns
348 controlling rainfall and floods into the Dead Sea: Implications for the lake's sedimentology

- 349 and paleohydrology. *Quaternary Science Reviews*, 216, 58–73,
350 doi:10.1016/j.quascirev.2019.06.005
- 351 Avanzi, F., De Michele, C., Gabriele, S., Ghezzi, A., & Rosso, R. (2015). Orographic Signature
352 on Extreme Precipitation of Short Durations. *J. Hydrometeorol.*, 16, 278–294,
353 doi:10.1175/JHM-D-14-0063.1
- 354 Bonacina, L. C. W. (1945), Orographic rainfall and its place in the hydrology of the globe.
355 *Quarterly Journal of the Royal Meteorological Society*, 71, 41–55,
356 doi:10.1002/qj.49707130705
- 357 Bongioannini Cerlini, P., Emanuel, K. A., & Todini, E. (2005). Orographic effects on convective
358 precipitation and space-time rainfall variability: preliminary results. *Hydrol. Earth Syst. Sci.*,
359 9, 285–299, doi:10.5194/hess-9-2285-2005
- 360 Borga, M., Stoffel, M., Marchi, L., Marra, F., & Jacob M. (2014), Hydrogeomorphic response to
361 extreme rainfall in headwater systems: flash floods and debris flows. *J. Hydrol.*, 518, 194–
362 205, doi:10.1016/j.jhydrol.2014.05.022
- 363 Buishand, T.A., 1991. Extreme rainfall estimation by combining data from several sites. *Hydrol.*
364 *Sci. J.*, 36 (4), 345–365, doi:10.1080/02626669109492519.
- 365 Burlando, P., & Rosso, R. (1996), Scaling and multiscaling models of depth-duration-frequency
366 curves for storm precipitation. *Journal of Hydrology*, 187, 45–64. Doi:10.1016/S0022-
367 1694(96)03086-7
- 368 Ceresetti, D., Molinié, G., & Creutin, J.-D. (2010), Scaling properties of heavy rainfall at short
369 duration: A regional analysis. *Water Resources Research*, 46, W09531.
370 doi:10.1029/2009WR008603
- 371 Chow, V., Maidment, D., & Mays, L. (1988). *Applied hydrology* (1st ed.). New York: McGraw-
372 Hill Science/Engineering/Math.
- 373 Dacre, H. F., Clark, P. A., Martinez-Alvarado, O., Stringer, M. A. and Lavers, D. A. (2015),
374 How do atmospheric rivers form?, *Bull. Am. Meteorol. Soc.*, 96(8), 1243–1255,
375 doi:10.1175/BAMS-D-14-00031.1
- 376 Fatichi, S., Ivanov, V. Y., Paschalis, A., Peleg, N., Molnar, P., Rimkus, S., Kim, J., Burlando, P.,
377 & Caporali, E. (2016), Uncertainty partition challenges the predictability of vital details of
378 climate change. *Earth's Future* 4(5), 240–251

- 379 Furcolo, P., Pelosi, A., & Rossi, F. (2016), Statistical identification of orographic effects in the
380 regional analysis of extreme rainfall. *Hydrological Processes*, 30, 1342–1353,
381 doi:10.1002/hyp.10719
- 382 Haan, C. T. (2002), *Statistical methods in hydrology*, 2nd ed., 496 pp., Iowa State Univ. Press,
383 Iowa
- 384 Haiden, T., Kerschbaum, M., Kahlig, P., & Nobilis, F. (1992). A refined model of the influence
385 of orography on the mesoscale distribution of extreme precipitation. *Hydrological Sciences*
386 *Journal*, 37, 5, 417-427
- 387 Houze, R. A., Jr, James, C. N. & Medina, S. (2001). Radar observations of precipitation and
388 airflow on the Mediterranean side of the Alps: Autumn 1998 and 1999. *Q. J. R. Meteorol.*
389 *Soc.*, 127, 2537-2558. doi:10.1002/qj.49712757804
- 390 Kushnir, Y., Dayan, U., Ziv, B., Morin, E., & Enzel, Y. (2017), Climate of the Levant:
391 phenomena and mechanisms. In Y. Enzel & B.-Y. Ofer (Eds.), *Quaternary of the Levant:*
392 *environments, climate change, and humans (pp. 31–44)*. Cambridge, UK: Cambridge
393 University Press
- 394 Marani, M., & Ignaccolo, M. (2015), A metastatistical approach to rainfall extremes. *Advances*
395 *in Water Resources*, 79, 121–126. doi:10.1016/j.advwatres.2015.03.001
- 396 Marra, F., Borga, M., & Morin, E. (2020), A unified framework for extreme sub-daily
397 precipitation frequency analyses based on ordinary events. *Geophys. Res. Lett.*, 47, 18,
398 e2020GL090209, doi:10.1029/2020GL090209
- 399 Marra, F., & Morin, E. (2015), Use of radar QPE for the derivation of Intensity–Duration–
400 Frequency curves in a range of climatic regimes. *J. Hydrol.*, 531, 427-440,
401 doi:10.1016/j.jhydrol.2015.08.064
- 402 Marra, F., Nikolopoulos, E. I., Anagnostou, E. N., & Morin, E. (2018), Metastatistical extreme
403 value analysis of hourly rainfall from short records: Estimation of high quantiles and impact
404 of measurement errors. *Adv. Water Resour.*, 117, 27–39,
405 doi:10.1016/j.advwatres.2018.05.001
- 406 Marra, F., Zocatelli, D., Armon, M., & Morin, E. (2019), A simplified MEV formulation to
407 model extremes emerging from multiple nonstationary underlying processes. *Adv. Water*
408 *Resour.*, 127, 280-290, doi:10.1016/j.advwatres.2019.04.002

- 409 Miniussi, A., Villarini, G., & Marani, M. (2020), Analyses through the metastatistical extreme
410 value distribution identify contributions of tropical cyclones to rainfall extremes in the
411 eastern United States. *Geophys. Res. Lett.*, *47*, e2020GL087238, doi:10.1029/2020GL087238
- 412 Nykanen, D. K., & Harris, D. (2003), Orographic influences on the multiscale statistical
413 properties of precipitation, *J. Geophys. Res.*, *108(D8)*, 8381, doi:10.1029/2001JD001518
- 414 Papalexiou, S. M. (2018), Unified theory for stochastic modelling of hydroclimatic processes:
415 Preserving marginal distributions, correlation structures, and intermittency. *Advances in*
416 *Water Resources*, *115*, 234–252, doi:10.1016/j.advwatres.2018.02.013
- 417 Papalexiou, S. M., AghaKouchak, A., & Foufoula-Georgiou, E. (2018), A diagnostic framework
418 for understanding climatology of tails of hourly precipitation extremes in the United States.
419 *Water Resources Research*, *54*, doi:10.1029/2018WR022732
- 420 Peleg, N., & E. Morin (2012), Convective rain cells: Radar-derived spatiotemporal
421 characteristics and synoptic patterns over the eastern Mediterranean, *J. Geophys. Res.*, *117*,
422 D15116, doi:10.1029/2011JD017353
- 423 Picard, L. & Mass, C. (2017), The sensitivity of orographic precipitation to flow direction: An
424 idealized modeling approach. *J. Hydrometeorol.* *18*, 1673–1688, doi:10.1175/JHM-D-16-
425 0209.1
- 426 Restrepo-Posada, P. J., & Eagleson, P. S. (1982), Identification of independent rainstorms,
427 *Journal of Hydrology*, *55*, 303–319, doi:10.1016/0022-1694(82)90136-6
- 428 Roe, G. H. (2005), Orographic precipitation. *Annu. Rev. Earth Planet. Sci.*, *33*, 645–71, doi:
429 10.1146/annurev.earth.33.092203.122541
- 430 Rossi, M. W., Anderson, R. S., Anderson, S. P., & Tucker, G. E. (2020), Orographic controls on
431 subdaily rainfall statistics and flood frequency in the Colorado Front Range, USA.
432 *Geophysical Research Letters*, *47*, e2019GL085086, doi:10.1029/2019GL085086
- 433 Toreti, A., Giannakaki, P. & Martius, O. (2016), Precipitation extremes in the Mediterranean
434 region and associated upper-level synoptic-scale flow structures. *Clim. Dyn.*, *47*, 1925–1941,
435 doi:10.1007/s00382-015-2942-1
- 436 de Vries, A.J., Tyrlis, E., Edry, D., Krichak, S.O., Steil, B., & Lelieveld, J. (2013), Extreme
437 precipitation events in the Middle East: dynamics of the Active Red Sea Trough. *J. Geophys.*
438 *Res. Atmos.* *118*, 7087–7108, doi:10.1002/jgrd.50569

439 Zorretto, E., Botter, G., & Marani, M. (2016), On the emergence of rainfall extremes from
440 ordinary events. *Geophysical Research Letters*, 43, 8076–8082, doi:10.1002/2016GL069445